Determination of the isotopic composition of gadolinium using multicollector inductively coupled plasma mass spectrometry

He, Juan; Yang, Lu; Hou, Xiandeng; Mester, Zoltan; Meija, Juris

Publisher's version / Version de l'éditeur:
https://doi.org/10.1021/acs.analchem.0c00531
Analytical Chemistry, 92, 8, pp. 6103-6110, 2020-04-21

analytical chemistry

pubs.acs.org/ac Article

Determination of the Isotopic Composition of Gadolinium Using Multicollector Inductively Coupled Plasma Mass Spectrometry

Juan He, Lu Yang,* Xiandeng Hou, Zoltan Mester, and Juris Meija

Cite This: *Anal. Chem.* 2020, 92, 6103−6110 Read Online

ABSTRACT: In this study, we report independent measurements of all stable isotope ratios of gadolinium. Our study employs multicollector inductively coupled plasma mass spectrometry (MC-ICPMS) with National Research Council Canada (NRC) HALF-1 isotopic hafnium standard as a primary calibrator and surveys four commercial gadolinium materials, including a NRC candidate isotopic reference material, GADS-1. The isotopic composition of gadolinium is determined using the regression model without reliance on conventional normalizing isotope ratios or mass-dependent isotope ratio correction models. In this work, all gadolinium isotope ratios were obtained from $^{160}Gd/^{158}Gd$ which, in turn, was measured from hafnium $^{178}Hf/^{177}Hf$ either directly or indirectly through $^{167}Er/^{166}Er$. The latter approach was used for the final determination of gadolinium isotopic composition, as it provides smaller combined uncertainty. We report high-precision measurements of the isotopic composition of gadolinium, which support a revised standard atomic weight. Isotope amount ratios of $R_{152/158}$ = 0.008 20(2)$_{k=1}$, $R_{154/158}$ = 0.087 98(12)$_{k=1}$, $R_{155/158}$ = 0.596 81(63)$_{k=1}$, $R_{156/158}$ = 0.825 08(57)$_{k=1}$, $R_{157/158}$ = 0.630 60(22)$_{k=1}$, and $R_{160/158}$ = 0.879 10(60)$_{k=1}$, and the atomic weight of A_r(Gd) = 157.2502(6)$_{k=1}$ were obtained for gadolinium in GADS-1.

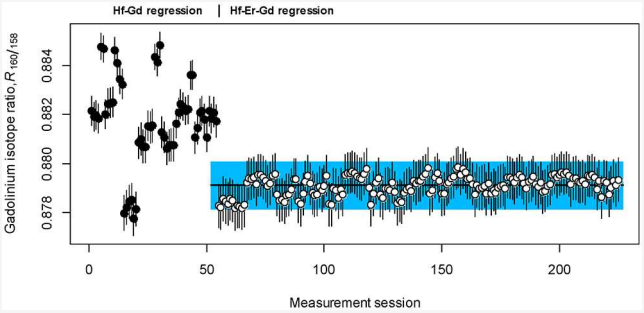

Isotopes of gadolinium display several unique physical properties, which lead to numerous applications.[1] As an example, ^{155}Gd and ^{157}Gd have large absorption cross-section for thermal neutrons thus making them effective in controlling nuclear reactors.[1−4] In this vein, changes of gadolinium isotopic composition are used to monitor the nuclear fuel during fission reactions.[3,5] Gadolinium isotopes also have applications in geoscience because variations of $^{156}Gd/^{155}Gd$ and $^{158}Gd/^{157}Gd$ isotope amount ratios can be used to study thermal neutron capture[6,7] or the interaction of cosmic rays with planetary materials.[6,8−10] Owing to its magnetic properties, gadolinium finds widespread use in neutron capture therapy (Gd-NCT) for cancer treatment[11−19] and as a contrast agent in magnetic resonance imaging (MRI).[20−23] Given that the applications of gadolinium are isotope-specific, analysis of gadolinium isotope ratios are crucial in medical applications.[24] Moreover, with the increased use of Gd-based materials in nuclear industry, medicine, and technology, gadolinium has emerged as a contaminant of aquatic environments which will place even greater demands for its analysis.[25−27]

Despite its importance, gadolinium remains one of the few elements whose isotopic composition has received little attention. Indeed, the International Union of Pure and Applied Chemistry (IUPAC) recently noted that new calibrated isotopic composition measurements of gadolinium could substantially improve its standard atomic weight.[28] Both thermal ionization mass spectrometry (TIMS) and multi-collector inductively coupled plasma mass spectrometry (MC-ICPMS) have been used for gadolinium isotope ratio measurements for decades. However, in the absence of gadolinium isotope standards, all studies thus far have relied on conventional values for isotope ratios to correct for instrumental isotopic fractionation, for example, by assuming that $^{156}Gd/^{160}Gd$ = 0.9361 in all materials for some reason—an assumption that has been shown invalid.[29] The aim of this study is to provide an independent calibrated measurement of isotopic composition of gadolinium without relying on any such conventional isotope ratio normalizing values. A primary method of isotope amount ratio analysis is the full gravimetric isotope mixture (FGIM) model, which requires weighable amounts of all near-pure (separated) isotopes of the element.[30] Such method is costly for gadolinium, having seven isotopes. A low-cost alternative approach, employed in this work, is the regression model, which is increasingly employed for absolute isotope amount ratio measurements.[31−37] This model enables

Received: February 6, 2020
Accepted: March 27, 2020
Published: April 8, 2020

https://dx.doi.org/10.1021/acs.analchem.0c00531
Anal. Chem. 2020, 92, 6103−6110

performing calibrated isotope ratio measurements of an element using isotopic standard of another element.

■ EXPERIMENTAL SECTION

Instrumentation. A Neptune Plus MC-ICPMS (Thermo Fisher Scientific, Bremen, Germany) was used for isotope ratio measurements in low mass-resolution mode. Our MC-ICPMS has nine Faraday cups and a quartz dual cyclonic spray chamber with a plastic (PFA) self-aspirating nebulizer (Elemental Scientific; Omaha NE, USA) operating at 50 μL min^{-1}. The instrument was tuned for high sensitivity, while maintaining flat-top square peaks and stable signals. The gain calibration of the Faraday cups was performed weekly to ensure the normalization of their efficiencies and rotating amplifiers were used. Typical operating conditions are presented in Table 1.

Table 1. MC-ICPMS Operating Condition

instrument settings	
radio frequency power	1250−1305 W
plasma gas flow rate	16.0 L min^{-1}
auxiliary gas flow rate	1.00 L min^{-1}
sample gas flow rate	1.010−1.020 L min^{-1}
sampler cone orifice (Ni)	1.1 mm
skimmer cone orifice (H, Ni)	0.8 mm
lens settings	optimized for maximum and stable signal while maintaining a flat top peak
data acquisition parameters	
Faraday cup configuration 1 (Hf → Gd)	L3 (^{158}Gd), L2 (^{160}Gd), C (^{167}Er), H3 (^{177}Hf), H4 (^{178}Hf)
Faraday cup configuration 2 (Hf → Er)	L4 (^{166}Er), L3 (^{167}Er), C (^{177}Hf), H1 (^{178}Hf)
Faraday cup configuration 3 (Er → Gd)	L1 (^{158}Gd), C (^{160}Gd), H2 (^{166}Er), H3 (^{167}Er)
Faraday cup configuration 4 (Gd → Gd)	L3 (^{152}Gd), L2 (^{154}Gd), L1 (^{155}Gd), C (^{156}Gd), H2 (^{157}Gd), H2 (^{158}Gd), H3 (^{160}Gd), H4 (^{161}Dy)
mass resolution	low
signal integration time	2.097 s
number of integrations, cycles, and blocks	1, 8, 7 (Gd−Gd); 1, 12, 5 (Hf−Gd); 1, 12, 4 (Hf−Er and Er−Gd)

Reagents and Solutions. High-purity nitric acid was obtained by a sub-boiling distillation system (Milestone Inc.; Shelton CT, USA) of reagent grade feedstock (Fisher Scientific; Ottawa ON, Canada). High purity (18.5 MΩ cm) deionized water was obtained from a Milli-Q ion exchange system (Sigma-Aldrich; Oakville ON, Canada). All labware was cleaned in 5% HNO_3 solution and rinsed with deionized water prior use. All acids and standard solutions were prepared under class 100 clean laboratory conditions.

All gadolinium standards were obtained from commercial vendors. The Gd-1 standard solution (∼1000 mg L^{-1} in 2% HNO_3) was sourced from Sigma-Aldrich (Oakville ON, Canada); the Gd-2 standard solution (∼1000 mg L^{-1} in 4% HNO_3) was purchased from SCP Science (Baie-D'Urfé QC, Canada), and the Gd-3 standard solution (∼1000 mg L^{-1} in 7% HNO_3) was obtained from Delta Scientific (ISOSPEC Gd; Ottawa ON, Canada). The Gd-4 standard solution (∼10 000 mg L^{-1} in 5% HNO_3) was sourced from Alfa Aesar (Tewksbury MA, USA). All four of these solutions were prepared from Gd_2O_3, and Gd-4 was diluted 10-fold in 2% HNO_3 to produce isotopic reference material NRC GADS-1.

The primary isotope ratio calibrator employed in this work was a Certified Reference Material (CRM) of hafnium (HALF-1; National Research Council Canada, Ottawa ON, Canada)[35] and erbium standard solution (Specpure, prepared from Er_2O_3) at ∼10 000 mg kg^{-1} in 5% HNO_3 was purchased from Fisher Scientific (Ottawa, ON, Canada).

Sample Preparation and Analysis. Solutions containing mixture of Hf−Gd, Hf−Er, and Er−Gd were prepared by diluting the individual stock solutions of Gd (Gd-4 or GADS-1), Hf (HALF-1), and Er (Specpure) in 1% HNO_3 resulting in mass fractions w(Gd) = 5.0−5.5 mg kg^{-1}, w(Hf) = 3.0−3.5 mg kg^{-1}, and w(Er) = 3.0−3.5 mg kg^{-1}.

A self-aspiration mode was used for the sample introduction at a flow rate of 50 μL min^{-1}. Similar to previous studies,[32−37] the instrument plasma radio frequency (RF) power was increased stepwise (four steps) from the optimum value P_0 (which corresponds to the highest sensitivity region, stable signal, and flat top peak, typically at 1250 W) to P_{max} (typically at 1310 W), wherein Gd, Hf, and Er signals decreased by approximately 25−30% compared to their values at P_0. The purpose of this deliberate plasma RF power change during the measurement session is to induce a fast drift in the mass bias. Each session of measurement takes ∼15 min (compared to several hours when the mass bias drift is not induced deliberately[30]). The isotope ratios of all samples were measured by incrementally increasing RF power with values of $P = (P_{max} - P_0)\cdot N/4$, where N = 0, 1, 2, 3, and 4 for each measurement session, which forms a linear regression data set (Figure 1). Signals of all measured isotopes obtained from a blank solution of 1% HNO_3 at the optimum RF power were subtracted from all measurement results for simplicity. In principle, the corresponding blank should be subtracted for the sample at each RF value. Since intensities of all measured isotopes in the blank at P_0 were very small (0.06−1.0 mV) compared to intensities in the samples (17−40 V), both blank

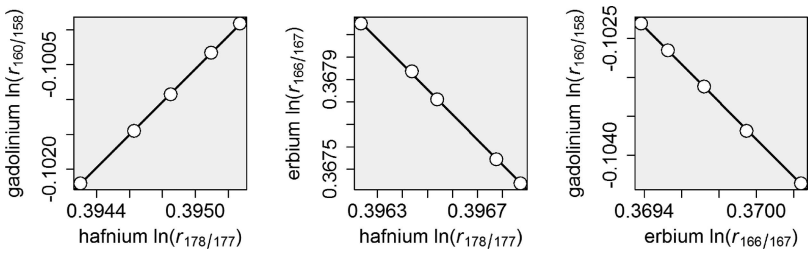

Figure 1. Typical MC-ICPMS log−linear regression plots of Hf → Gd (R^2 = 0.9999), Hf → Er (R^2 = 1.0000), and Er → Gd (R^2 = 1.0000) isotope ratios. Repeatability uncertainty of isotope ratios is smaller than the symbols.

https://dx.doi.org/10.1021/acs.analchem.0c00531
Anal. Chem. 2020, 92, 6103−6110

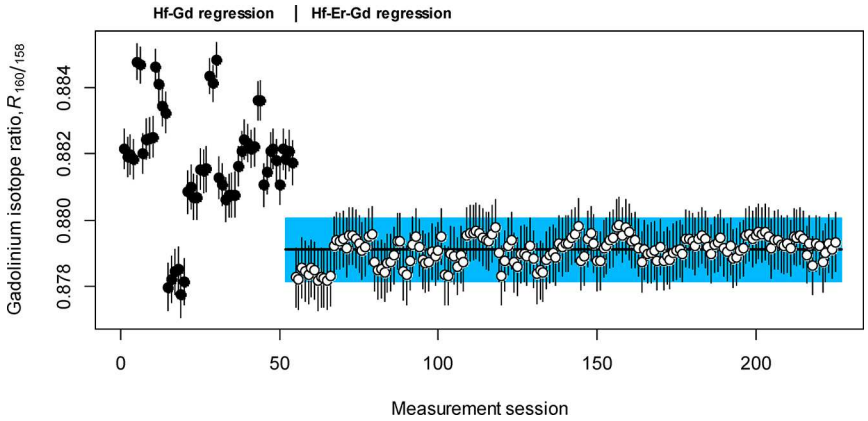

Figure 2. Measurement results of gadolinium isotope ratio $R_{160/158}$ in the isotopic standard, NRC GADS-1, using regression model. Comparison of a one-step direct approach Hf → Gd with a two-step indirect approach (Hf → Er → Gd). Vertical error bars represent standard uncertainty, which includes contribution from the primary hafnium standard (NRC HALF-1), and shaded rectangle represents the uncertainty of the consensus value of $R_{160/158}$ in GADS-1.

subtraction approaches yields identical isotope ratios. Static run was employed for isotope ratio measurements, as shown in Table 1. The quality of each data set was monitored via the linear correlation coefficient (R^2) which was always $R^2 > 0.9995$. Results reported in this study were collected at the NRC between November 2018 and August 2019.

Spectral Interferences. Individual stock solutions of Gd, Er, and Hf were prepared from high purity materials to avoid any potential spectral interferences (Table S1). However, potential isobaric interferences from $^{152}Sm^+$, $^{154}Sm^+$, $^{156}Dy^+$, $^{158}Dy^+$, and $^{160}Dy^+$ on Gd isotopes could occur in samples containing these elements affecting the accuracy of gadolinium isotope amount ratios. For mass bias calibration, interference-free major isotopes of erbium and hafnium (^{166}Er, ^{167}Er, ^{177}Hf, ^{178}Hf) were selected. Quantitative analysis of sample solutions containing 5 mg kg^{-1} gadolinium with HR-ICPMS (element) using external calibration showed Sm to be present at levels below 5 ng kg^{-1} and Dy at 0.7 μg kg^{-1}. The mass fraction of Sm in the Gd test solutions is insignificant to form isobaric interferences since the mass fraction of gadolinium in the analyzed samples are several orders of magnitude higher (5 mg kg^{-1}). Since the interference from Dy on Gd isotopes could affect the accuracy of gadolinium isotope ratios, a 10^{13} Ω resistor was used for the Faraday cup H4 to measure $^{161}Dy^+$. Note that cross gain calibration of Faraday cup with 10^{13} Ω resistor to normal 10^{11} Ω resistor was performed weekly to ensure the normalization of their efficiencies following the manufacturer's recommendation. A 5 mg kg^{-1} test solution of gadolinium produced 0.0015 V signal for ^{161}Dy compared to 42 V for ^{160}Gd. Such amounts of Dy are insignificant to affect gadolinium isotope signals, and no correction for Dy was performed.

■ RESULTS AND DISCUSSION

Correction for Instrumental Isotopic Fractionation (Mass Bias). The regression model allows to perform calibrated isotope amount ratio measurements of an element with the use of isotopic standard of another element. The method is based on the observed correlated drift in isotope amount ratios of two elements in MC-ICPMS as expressed by eq 1 for the Hf → Gd system:[30]

$$\ln r^{Gd}_{160/158}(t) = a + b \cdot \ln r^{Hf}_{178/177}(t) \quad (1)$$

The coefficients a and b are obtained using the least-squares fitting of data. The mass bias (K) is defined as the ratio of the corrected and measured isotope amount ratios ($K = R/r$). Assuming that the log ratio of the individual fractionation coefficients ($\ln K_{160/158}/\ln K_{178/177}$) remains constant during the measurement, the mass bias corrected isotope ratio of gadolinium can be obtained

$$\ln R^{Gd}_{160/158} = a + b \cdot \ln R^{Hf}_{178/177} \quad (2)$$

As detailed elsewhere,[30] this regression model effectively calibrates each isotope amount ratio of the analyte element from the known isotope amount ratio of a calibrator element without assuming that these two elements undergo identical instrumental fractionation. Also note that this regression formalism involves two-parameters (intercept and slope) unlike the early formulations with constrained intercept.[38,39] In addition, the analyte and the calibrator are both measured simultaneously from the same solution thus eliminating sample matrix effects. This optimized regression model has been validated. First, the use of two independent calibrators (Re and Tl) produced identical iridium isotope amount ratios to within few parts in 10^4.[32] Second, the regression model has been compared with the full gravimetric isotope mixture method (a primary method) in molybdenum[31] and lead[34] isotope ratio measurements, both showing excellent agreement between the results to within few parts in 10^4. This state-of-the-art optimized regression model has been employed in a number of studies by various research groups[31−37] and is currently the best approach to perform isotope amount ratio measurements for many elements.

Measurement Strategy. Although the regression model does not require identical mass bias between the analyte and calibrator isotope amount ratios, we have found previously that better results are obtained when both elements are close in mass.[32] Thus, Eu or Er would be good calibrators for Gd. Unfortunately, such standards are not available and the closest isotopic standard available on the market is hafnium isotopic standard HALF-1 (NRC Canada). Because of the Faraday cup arrangement in our instrument, it is impossible to simultaneously collect all seven isotopes of gadolinium along with ^{177}Hf and ^{178}Hf in the static mode (which provides best performance). As a result, we have employed two different calibration strategies. First, we used NRC HALF-1 to directly

https://dx.doi.org/10.1021/acs.analchem.0c00531
Anal. Chem. 2020, 92, 6103−6110

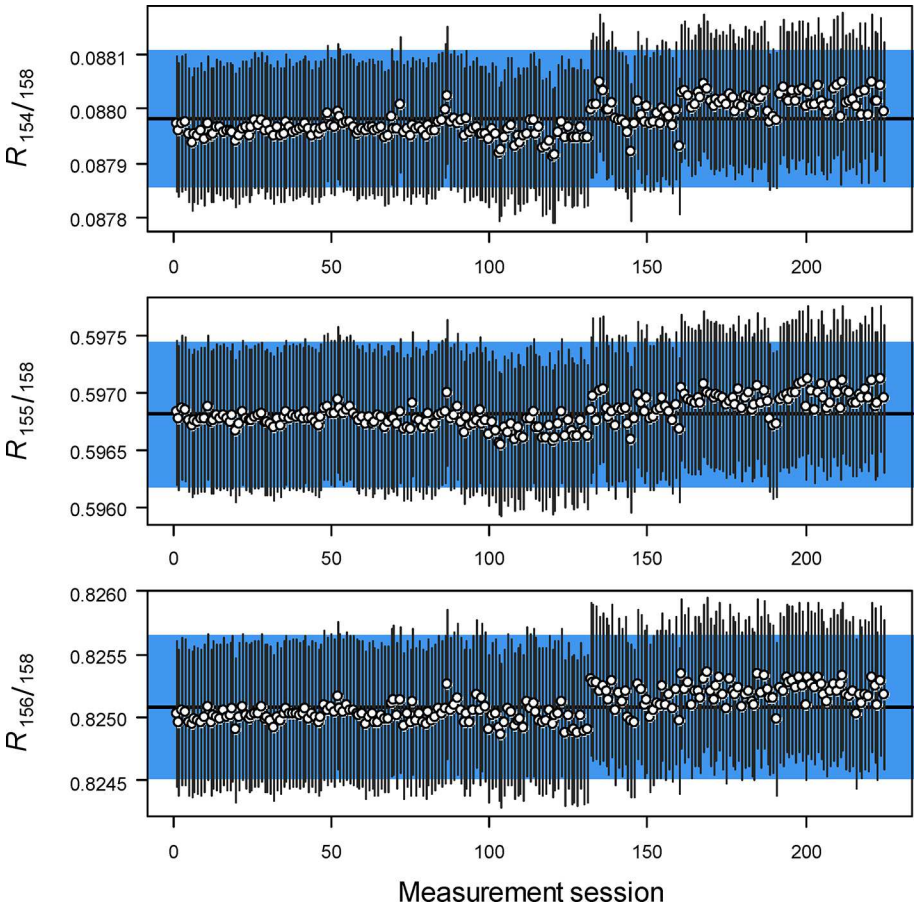

Figure 3. Gadolinium isotope ratios for NRC GADS-1 using MC-ICPMS and a three-step $^{178}Hf/^{177}Hf \rightarrow {}^{166}Er/^{167}Er \rightarrow {}^{160}Gd/^{158}Gd \rightarrow {}^{A}Gd/^{158}Gd$ regression method to correct instrumental isotopic fractionation effects (mass bias). Measurements shown in this figure were acquired over the period of 8 months. Error bars represent combined standard uncertainties which include contributions from hafnium calibrator (NRC HALF-1).

calibrate $^{160}Gd/^{158}Gd$, which, in turn, was used to calibrate all other Gd isotope amount ratios. The second approach first calibrated $^{166}Er/^{167}Er$ ratio from $^{178}Hf/^{177}Hf$, which was then used to calibrate $^{160}Gd/^{158}Gd$, and subsequently all other Gd isotope amount ratios. Isotope ratio $^{166}Er/^{167}Er$ was selected by considering the abundance of isotopes and the ability to establish static Faraday cup configuration for measuring gadolinium isotopes or hafnium isotopes along with the two chosen erbium isotopes. A total of 600+ regression sets were obtained: Hf → Gd (54 sets), Hf → Er (186 sets), Er → Gd (171 sets), and Gd → Gd (225 sets) over a course of one year.

It is possible for more intermediate steps to be employed, such as Hf → Yb → Er → Gd. But as the number of steps increases so does the instrument time and cost without a guarantee that the final uncertainty of gadolinium isotope amount ratios remains sufficiently low.

Using the direct Hf → Gd approach to calibrate $^{160}Gd/^{158}Gd$ ratio seems like a better alternative to the indirect two-step approach Hf → Er → Gd. Indeed, the average uncertainty of individual $^{160}Gd/^{158}Gd$ estimates from the direct approach is nearly twice smaller than those from the indirect approach. However, the results of the direct approach show a significant overdispersion compared to those of the indirect approach (see Figure 2). This means that the lower uncertainties from Hf → Gd do not capture some yet-to-be-explained source of uncertainty (this is formally known as the dark uncertainty). In the contrast, the larger uncertainties from the Hf → Er → Gd seem to adequately reflect the spread of data from the long-term results. This observation supports our previous findings,[32] which favor closer distance between the mass of the analyte and the calibrator. Thus, when the regression model is employed, selecting a calibrator that is closest to the analyte in mass is important to ensure reliable measurements. Subsequently, the indirect approach Hf → Er → Gd was selected for the final determination of $^{160}Gd/^{158}Gd$ isotope amount ratio.

Uncertainty Evaluation. Uncertainty evaluation of gadolinium isotope amount ratios was done as outlined in our previous study.[37] First, the linear fits were obtained on all 600+ data sets using ordinary least-squares. As an example, the Hf → Er regression coefficients a_{Hf-Er} and b_{Hf-Er} are obtained by solving the following statistical expression for the unknown variables u_{Er}, a_{Hf-Er}, and b_{Hf-Er}:

$$\ln(r^{Er}_{166/167}) \sim N(a_{Hf-Er} + b_{Hf-Er} \times \ln(r^{Hf}_{178/177}), u_{Er}) \quad (3)$$

The notation $z \sim N(\alpha, \sigma)$ means that a data point z is interpreted as a random draw from a Gaussian (normal) distribution with mean α and standard deviation σ. The obtained regression parameters were then transformed into the corresponding isotope ratios as per eq 2. As an example, the Hf → Er regressions would provide 186 estimates of $^{166}Er/^{167}Er$ isotope ratio, $p^{Er}_{166/167}$, which are calculated as follows:

https://dx.doi.org/10.1021/acs.analchem.0c00531
Anal. Chem. 2020, 92, 6103−6110

$$\ln(p^{\mathrm{Er}}_{166/167}) = a_{\mathrm{Hf-Er}} + b_{\mathrm{Hf-Er}} \times \ln(R^{\mathrm{Hf}}_{178/177}) \quad (4)$$

There are many individual isotope ratio estimates, such as the 186 values for $p^{\mathrm{Er}}_{166/167}$ from all Hf → Er regressions or the 171 values of $p^{\mathrm{Gd}}_{166/167}$ from all Er → Gd regressions are combined into single consensus values using the random effects model. This model is chosen to capture the variability between the individual measurement sets which is most evident from the 54 sets of Hf → Gd regressions shown in Figure 2.

The consensus isotope amount ratio values of erbium and gadolinium, $R^{\mathrm{Er}}_{166/167}$ and $R^{\mathrm{Gd}}_{A/158}$ are obtained using random effects model from the estimates $p^{\mathrm{Er}}_{166/167}$ and $p^{\mathrm{Gd}}_{A/158}$:

$$p^{\mathrm{Er}}_{166/167} \sim N(R^{\mathrm{Er}}_{166/167}, t_{\mathrm{Hf-Er}}) \quad (5)$$

$$p^{\mathrm{Gd}}_{160/158} \sim N(R^{\mathrm{Gd}}_{160/158}, t_{\mathrm{Er-Gd}}) \quad (6)$$

$$p^{\mathrm{Gd}}_{A/158} \sim N(R^{\mathrm{Gd}}_{160/158}, t_{\mathrm{Gd-Gd},A}) \text{ for } A = 152, 154 - 157 \quad (7)$$

The Hf → Gd regressions were not used in the consensus building. Isotopic abundances and the atomic weight of gadolinium were obtained from the corresponding isotope amount ratio consensus values and their uncertainties while taking into the account covariances between the isotope amount ratios.[40,41] The results of this study are traceable to NRC HALF-1 hafnium standard with isotope ratio $R^{\mathrm{Hf}}_{178/177}$ = 1.4689 having standard uncertainty $u(R^{\mathrm{Hf}}_{178/177})$ = 0.0004. We estimate that the uncertainty of ^{160}Gd/^{158}Gd isotope ratio in GADS-1 standard was largely due to NRC HALF-1 primary standard (40%) and session-to-session reproducibility (60%).

Measurement Results for GADS-1 Standard. The ^{160}Gd/^{158}Gd ratio in GADS-1 obtained from the two-step Hf → Er → Gd regression method was used to calibrated all other gadolinium isotope ratios using a third regression step involving only gadolinium isotopes. Measurements of the GADS-1 standard were performed from solutions with w(Gd) = 5.0−5.5 mg kg^{-1} over nine months during which six sets of MC-ICPMS cones were used and 225 sets of Gd → Gd regressions were obtained (Figure 3). The calibrated isotope ratios of gadolinium were used to calculate the corresponding isotopic abundances and atomic weight:

$$x_i = \frac{R_{i/158}}{\sum_j R_{j/158}} \quad (8)$$

$$A_{\mathrm{r}}(\mathrm{Gd}) = \sum_i m_i x_i \quad (9)$$

The atomic masses of gadolinium isotopes used for calculations in this study are from the 2016 Atomic Mass Evaluation report[42] and are listed in Table S2. The resulting consensus values of the isotopic composition are summarized in Table 2. The atomic weight of gadolinium in the NRC GADS-1 standard, A_{r}(Gd, GADS-1) = 157.2502(6), agrees well with the current standard atomic weight 157.25 ± 0.03.[43] Note that the value reported in the parentheses is the standard uncertainty of our result, $u(A_{\mathrm{r}}(\mathrm{Gd, GADS\text{-}1}))$ = 0.0006. We also note that our work provides an estimate of ^{166}Er/^{167}Er isotope ratio in our measurement standard $R_{166/167}$ = 1.4635(4). Our work also provides an estimate of ^{156}Gd/^{160}Gd isotope ratio $R_{156/160}$ = 0.9386(9), which disagrees with the commonly used fixed value of 0.9361 at the 95% confidence.

Table 2. Isotopic Composition of Gadolinium in the NRC GADS-1 Standard[a]

atomic mass number, A	isotope ratio, $R_{A/158}$	isotopic abundance, x(^{A}Gd)
152	0.00820(2)	0.002036(4)
154	0.08798(12)	0.021844(30)
155	0.59681(63)	0.148173(140)
156	0.82508(57)	0.204848(120)
157	0.63060(22)	0.156564(60)
158	1 (exact)	0.248276(65)
160	0.87910(60)	0.218259(130)

[a]Notation $R_{160/158}$ = 0.87910(60) denotes a mean value $R_{160/158}$ = 0.87910 with standard uncertainty $u(R_{160/158})$ = 0.00060.

Comparison with Previous Work. The current standard atomic weight of gadolinium was adopted by IUPAC in 1955 based on isotopic abundance measurements by Hess (1948) and Leland (1950)[44] with further minor changes made in 1961 (isotope masses)[45] and 1969 (uncertainty evaluation).[46] Over the last 70 years, the measurement uncertainty has decreased by an order of magnitude making it clear that a survey of subsequent work is overdue. Table 3 provides a survey of gadolinium isotopic composition measurements.

Table 3. Survey of Gadolinium Atomic Weight Estimates

year	A_{r}(Gd)	lead author	ref
1948	157.250(6)	Hess[a]	47
1950	157.262(5)	Leland	48
1957	157.232(5)	Collins	49
1970	157.252(2)	Eugster	50
1981	157.252(2)	Holliger	51
1992	157.2486(4)	Dubois[b]	52
2020	157.2502(6)	this work	n/a

[a]No uncertainty is given for abundances, so they were taken to be same as in Leland (1950). [b]Uncertainty is evaluated by propagating the uncertainty of $R_{160/158}$, which was reported to be u = 0.000 22.

To the best of our knowledge, there is only one contemporary study, by Dubois et al.,[52] that reports isotopic measurements of gadolinium without relying on conventional values, such as ^{156}Gd/^{160}Gd = 0.9361, to correct instrumental isotope ratio fractionation. Dubois et al.[52] employed total evaporation TIMS for ^{157}Gd/^{158}Gd and ^{160}Gd/^{158}Gd with all other isotope ratios measured from these values using linear instrumental isotope fractionation model. Total evaporation TIMS is an established method for accurate isotope ratio measurements,[53−61] and our MC-ICPMS results are in agreement with this study at the 95% confidence level and have uncertainties of similar magnitude.

Isotope Delta Measurements of Gadolinium. Relative isotope ratios (isotope deltas) of gadolinium were performed against the GADS-1 standard using the combined standard-sample bracketing with europium as the internal standard.[30] Results are shown in Figure 4 from which we make two observations. First, albeit small, systematic mass-dependent variations can be seen between materials Gd-3 and GADS-1. Second, we note a large isotope delta $\delta_{\mathrm{GADS\text{-}1}}$($^{152/158}$Gd) = +0.59 ... + 0.74 ‰ in Gd-1 (range from ten replicate measurements). While it is tempting to interpret this anomalous isotope delta as samarium interference, we found <5 ng kg^{-1} levels of samarium in Gd-1, which can only account

https://dx.doi.org/10.1021/acs.analchem.0c00531
Anal. Chem. 2020, 92, 6103−6110

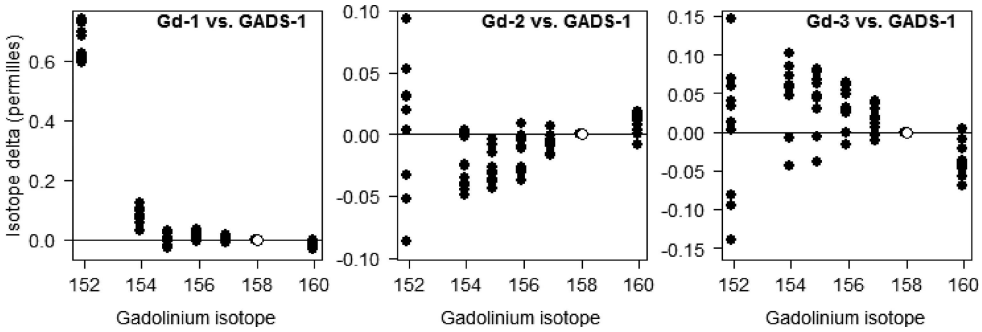

Figure 4. Isotope deltas of gadolinium in three commercial standards relative to NRC GADS-1.

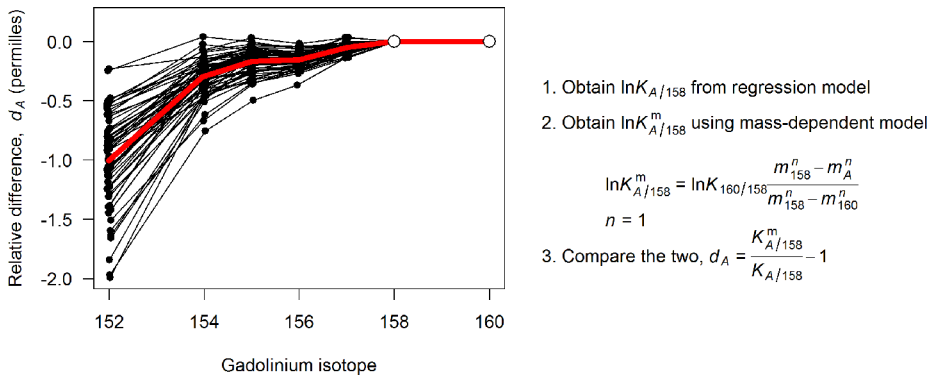

Figure 5. Comparison of the MC-ICPMS instrumental mass bias factors of gadolinium isotopes obtained from $K(^{160}Gd/^{158}Gd)$ using the regression model and the mass-dependent fractionation law.

for deviations in the gadolinium-152 signal in the order of few parts in 10^5 (0.1 ‰).

Mass-Independent Fractionation in MC-ICPMS. The lack of gadolinium isotopic standards[62] does not prevent doing gadolinium isotope ratio measurements. Typically, one adopts a conventional value, such as $^{156}Gd/^{160}Gd = 0.9361$, and a mathematical model to correct for instrumental fractionation of all isotope ratios with exponential law being the most common choice ($n = 1$):

$$\ln K(^{A}Gd/^{158}Gd) = \ln K(^{160}Gd/^{158}Gd) \times (m_{158}{}^{n} - m_{A}{}^{n}) / (m_{158}{}^{n} - m_{160}{}^{n}) \quad (10)$$

Unfortunately, many isotopes exhibit isotopic fractionation in MC-ICPMS whereby the magnitude of such fractionation cannot be explained with nuclide masses alone. This phenomenon is known as the mass-independent fractionation (MIF).[30] Recent studies report similar observations in TIMS for Fe and Ca isotopes.[63,64]

The regression model provides calibrated isotope amount ratios, and in turn, the correction factors $K(^{A}Gd/^{158}Gd)$, which we compare with the values calculated from $K(^{160}Gd/^{158}Gd)$ using the mass-dependent fractionation model (eq 10). Figure 5 shows the comparison of these two approaches for 225 sets of Gd → Gd regressions and one can make several observations from this plot. First, we note that the exponential model slightly under-corrects the instrumental isotopic fractionation (a value of $n = 0.7$ works significantly better for our data set). Second, there is significant day-to-day variability in the instrumental fractionation, which limits the precision of conventional mass bias correction to within parts per thousand.

CONCLUSION

Despite numerous applications of gadolinium isotopes, there has been only a single recent study devoted to the independent measurement of its isotopic composition (using total evaporation TIMS). Our work employs entirely different mass spectrometry (MC-ICPMS) and calibration approach, and the results are in agreement within their expanded uncertainties. The agreement between total evaporation TIMS and our MC-ICPMS results thus offers additional confidence in the cost-effective regression method for the determination of absolute isotope ratios of gadolinium. The MC-ICPMS results reported in this study are traceable to the International System of Units through the NRC HALF-1 hafnium isotopic standard and support a more precise standard atomic weight of gadolinium.

Our results also shed new light on the performance of the regression mass bias correction method, demonstrating the importance of selecting appropriate calibrator (Hf or Er for Gd) and the importance of capturing the session-to-session variability of the measurement results in the overall uncertainty budget.

ASSOCIATED CONTENT

Supporting Information

The Supporting Information is available free of charge at https://pubs.acs.org/doi/10.1021/acs.analchem.0c00531.

Possible spectral interferences of Gd, Er, and Hf isotopes and atomic masses of gadolinium isotopes (PDF)

Data file containing all measurement results (XLSX)

https://dx.doi.org/10.1021/acs.analchem.0c00531
Anal. Chem. 2020, 92, 6103−6110

AUTHOR INFORMATION

Corresponding Author

Lu Yang − *National Research Council Canada, Ottawa, Ontario K1A 0R6, Canada;* orcid.org/0000-0002-6896-8603; Email: lu.yang@nrc-cnrc.gc.ca

Authors

Juan He − *College of Chemistry, Sichuan University, Chengdu 610064, China; National Research Council Canada, Ottawa, Ontario K1A 0R6, Canada*

Xiandeng Hou − *Analytical & Testing Center, Sichuan University, Chengdu, Sichuan 610064, China;* orcid.org/0000-0003-2488-2063

Zoltan Mester − *National Research Council Canada, Ottawa, Ontario K1A 0R6, Canada;* orcid.org/0000-0002-2377-2615

Juris Meija − *National Research Council Canada, Ottawa, Ontario K1A 0R6, Canada*

Complete contact information is available at: https://pubs.acs.org/10.1021/acs.analchem.0c00531

Notes

The authors declare no competing financial interest.

ACKNOWLEDGMENTS

We thank The National Natural Science Foundation of China (Grant 21529501) and China Scholarship Council for financial support of J. He. during the study.

REFERENCES

(1) Dumazert, J.; Coulon, R.; Lecomte, Q.; Bertrand, G.; Hamel, M. *Nucl. Instrum. Methods Phys. Res., Sect. A* **2018**, *882*, 53−68.
(2) Oettingen, M.; Cetnar, J. *Nucl. Eng. Des.* **2014**, *273*, 359−366.
(3) Kim, J. S.; Jeon, Y. S.; Park, S. D.; Park, Y. J.; Ha, Y. K.; Song, K. *Asian J. Chem.* **2012**, *24* (7), 3274.
(4) Moreno, J. M. B.; Alonso, J. I. G.; Arbore, P.; Nicolaou, G.; Koch, L. *J. Anal. At. Spectrom.* **1996**, *11* (10), 929−935.
(5) Brennetot, R.; Becquet, A. L.; Isnard, H.; Caussignac, C.; Vailhen, D.; Chartier, F. *J. Anal. At. Spectrom.* **2005**, *20* (6), 500−507.
(6) Hidaka, H.; Ebihara, M.; Yoneda, S. *Earth Planet. Sci. Lett.* **2000**, *180* (1−2), 29−37.
(7) Hidaka, H.; Ebihara, M.; Yoneda, S. *Meteorit. Planet. Sci.* **2000**, *35* (3), 581−589.
(8) Hidaka, H.; Ebihara, M.; Yoneda, S. *Earth Planet. Sci. Lett.* **1999**, *173* (1−2), 41−51.
(9) Avila, J.; Ireland, T.; Lugaro, M.; Gyngard, F.; Karakas, A. Gadolinium and dysprosium isotopic compositions in stardust SiC grains from the murchison meteorite. *79th Annual Meeting of the Meteoritical Society*, 2016.
(10) Kuroda, P. *Geochem. J.* **1979**, *13* (6), 281−285.
(11) Shih, J. L. A.; Brugger, R. M. *Med. Phys.* **1992**, *19* (3), 733−744.
(12) Štefančíková, L.; Lacombe, S.; Salado, D.; Porcel, E.; Pagáčová, E.; Tillement, O.; Lux, F.; Depeš, D.; Kozubek, S.; Falk, M. *J. Nanobiotechnol.* **2016**, *14* (1), 63.
(13) Hosmane, N. S.; Maguire, J. A.; Zhu, Y. *Boron and Gadolinium Neutron Capture Therapy for Cancer Treatment*; World Scientific, 2012.
(14) Mowat, P.; Mignot, A.; Rima, W.; Lux, F.; Tillement, O.; Roulin, C.; Dutreix, M.; Bechet, D.; Huger, S.; Humbert, L.; et al. *J. Nanosci. Nanotechnol.* **2011**, *11* (9), 7833−7839.
(15) De Stasio, G.; Casalbore, P.; Pallini, R.; Gilbert, B.; Sanita, F.; Ciotti, M. T.; Rosi, G.; Festinesi, A.; Larocca, L. M.; Rinelli, A. *Cancer Res.* **2001**, *61* (10), 4272−4277.
(16) Hofmann, B.; Fischer, C.; Lawaczeck, R.; Platzek, J.; Semmler, W. *Invest. Radiol.* **1999**, *34* (2), 126−133.
(17) Miller, G. A., Jr; Hertel, N. E.; Wehring, B. W.; Horton, J. L. *Nucl. Technol.* **1993**, *103* (3), 320−331.
(18) Brugger, R.; Shih, J. *Strahlenther. Onkol.* **1989**, *165* (2/3), 153−156.
(19) Goorley, T.; Zamenhof, R.; Nikjoo, H. *Int. J. Radiat. Biol.* **2004**, *80* (11−12), 933−940.
(20) Darrah, T. H.; Prutsman-Pfeiffer, J. J.; Poreda, R. J.; Campbell, M. E.; Hauschka, P. V.; Hannigan, R. E. *Metallomics* **2009**, *1* (6), 479−488.
(21) Kamaly, N.; Pugh, J. A.; Kalber, T. L.; Bunch, J.; Miller, A. D.; McLeod, C. W.; Bell, J. D. *Mol. Imaging. Biol.* **2010**, *12* (4), 361−366.
(22) Caravan, P. *Chem. Soc. Rev.* **2006**, *35* (6), 512−523.
(23) Weinmann, H. J.; Brasch, R. C.; Press, W. R.; Wesbey, G. E. *AJR, Am. J. Roentgenol.* **1984**, *142* (3), 619−624.
(24) Bufalino, D.; Cerullo, N.; Colli, V.; Gambarini, G.; Rosi, G. *J. Phys.: Conf. Ser.* **2006**, *41*, 195.
(25) Knappe, A.; Möller, P.; Dulski, P.; Pekdeger, A. *Chem. Erde* **2005**, *65* (2), 167−189.
(26) Kulaksız, S.; Bau, M. *Appl. Geochem.* **2011**, *26* (11), 1877−1885.
(27) Blaum, K.; Geppert, C.; Schreiber, W.; Hengstler, J.; Müller, P.; Nörtershäuser, W.; Wendt, K.; Bushaw, B. *Anal. Bioanal. Chem.* **2002**, *372* (7−8), 759−765.
(28) Meija, J.; Coplen, T. B.; Berglund, M.; Brand, W. A.; De Bièvre, P.; Gröning, M.; Holden, N. E.; Irrgeher, J.; Loss, R. D.; Walczyk, T.; et al. *Pure Appl. Chem.* **2016**, *88* (3), 293−306.
(29) Hidaka, H.; Ebihara, M.; Shima, M. *Anal. Chem.* **1995**, *67* (8), 1437−1441.
(30) Yang, L.; Tong, S.; Zhou, L.; Hu, Z.; Mester, Z.; Meija, J. *J. Anal. At. Spectrom.* **2018**, *33* (11), 1849−1861.
(31) Malinovsky, D.; Dunn, P. J.; Goenaga-Infante, H. *J. Anal. At. Spectrom.* **2016**, *31* (10), 1978−1988.
(32) Zhu, Z.; Meija, J.; Zheng, A.; Mester, Z.; Yang, L. *Anal. Chem.* **2017**, *89* (17), 9375−9382.
(33) Zhu, Z.; Meija, J.; Tong, S.; Zheng, A.; Zhou, L.; Yang, L. *Anal. Chem.* **2018**, *90* (15), 9281−9288.
(34) Tong, S.; Meija, J.; Zhou, L.; Methven, B.; Mester, Z.; Yang, L. *Anal. Chem.* **2019**, *91* (6), 4164−4171.
(35) Tong, S.; Meija, J.; Zhou, L.; Mester, Z.; Yang, L. *Metrologia* **2019**, *56* (4), 044008.
(36) Zhang, R.; Meija, J.; Huang, Y.; Pei, X.; Mester, Z.; Yang, L. *Anal. Chim. Acta* **2019**, *1089*, 19−24.
(37) He, J.; Meija, J.; Hou, X. D.; Zheng, C. B.; Mester, Z.; Yang, L. *Anal. Bioanal. Chem.* **2019**, DOI: 10.1007/s00216-019-02271-6.
(38) Baxter, D. C.; Rodushkin, I.; Engström, E.; Malinovsky, D. *J. Anal. At. Spectrom.* **2006**, *21* (4), 427−430.
(39) Baxter, D. C.; Rodushkin, I.; Engström, E. *J. Anal. At. Spectrom.* **2012**, *27* (9), 1355−1381.
(40) Meija, J.; Mester, Z. *Metrologia* **2008**, *45* (1), 53.
(41) Meija, J.; Possolo, A. *Metrologia* **2017**, *54* (2), 229.
(42) Wang, M.; Audi, G.; Kondev, F.; Huang, W.; Naimi, S.; Xu, X. *Chin. Phys. C* **2017**, *41* (3), 030003.
(43) Meija, J.; Coplen, T. B.; Berglund, M.; Brand, W. A.; De Bièvre, P.; Gröning, M.; Holden, N. E.; Irrgeher, J.; Loss, R. D.; Walczyk, T.; et al. *Pure Appl. Chem.* **2016**, *88* (3), 265−291.
(44) Wichers, E. *J. Am. Chem. Soc.* **1956**, *78* (14), 3235−3240.
(45) Cameron, A. E.; Wichers, E. *J. Am. Chem. Soc.* **1962**, *84* (22), 4175−4197.
(46) Atomic Weights of the Elements 1969. *Pure Appl. Chem.* **1970**, *21*, 91.
(47) Hess, D. C., Jr. *Phys. Rev.* **1948**, *74* (7), 773.
(48) Leland, W. T. *Phys. Rev.* **1950**, *77* (5), 634.
(49) Collins, T.; Rourke, F.; White, F. *Phys. Rev.* **1957**, *105* (1), 196.
(50) Eugster, O.; Tera, F.; Burnett, D. S.; Wasserburg, G. J. *J. Geophys. Res.* **1970**, *75* (14), 2753−2768.
(51) Holliger, P.; Devillers, C. *Earth Planet. Sci. Lett.* **1981**, *52* (1), 76−84.
(52) Dubois, J.; Retali, G.; Cesario, J. *Int. J. Mass Spectrom. Ion Processes* **1992**, *120* (3), 163−177.

(53) Fujii, T.; Suzuki, D.; Watanabe, K.; Yamana, H. *Talanta* **2006**, *69* (1), 32−36.
(54) Richter, S.; Kühn, H.; Aregbe, Y.; Hedberg, M.; Horta-Domenech, J.; Mayer, K.; Zuleger, E.; Bürger, S.; Boulyga, S.; Köpf, A.; et al. *J. Anal. At. Spectrom.* **2011**, *26* (3), 550−564.
(55) Mathew, K.; O'Connor, G.; Hasozbek, A.; Kraiem, M. *J. Anal. At. Spectrom.* **2013**, *28* (6), 866−876.
(56) Mathew, K.; Haoszbek, A. *J. Radioanal. Nucl. Chem.* **2016**, *307* (3), 1681−1687.
(57) Fukami, Y.; Tobita, M.; Yokoyama, T.; Usui, T.; Moriwaki, R. *J. Anal. At. Spectrom.* **2017**, *32* (4), 848−857.
(58) Stanley, F.; Mathew, K.; Byerly, B.; Keller, R.; Spencer, K.; Thomas, M. *J. Radioanal. Nucl. Chem.* **2017**, *311* (3), 1819−1824.
(59) Wakaki, S.; Ishikawa, T. *Int. J. Mass Spectrom.* **2018**, *424*, 40−48.
(60) Quemet, A.; Ruas, A.; Dalier, V.; Rivier, C. *Int. J. Mass Spectrom.* **2019**, *438*, 166−174.
(61) Wang, S.; Wang, J.; Lu, H.; Fang, X.; Song, P.; Ren, T. *Rapid Commun. Mass Spectrom.* **2019**, *33* (9), 857−866.
(62) Isnard, H.; Brennetot, R.; Caussignac, C.; Caussignac, N.; Chartier, F. *Int. J. Mass Spectrom.* **2005**, *246* (1−3), 66−73.
(63) Fantle, M. S.; Bullen, T. D. *Chem. Geol.* **2009**, *258* (1−2), 50−64.
(64) Lehn, G. O.; Jacobson, A. D. *J. Anal. At. Spectrom.* **2015**, *30* (7), 1571−1581.

https://dx.doi.org/10.1021/acs.analchem.0c00531
Anal. Chem. 2020, 92, 6103−6110